Dear Referee #1,

Thank you for your comments and remarks. Below is our reply.

Lines 103-114: Please merge this chapter with introduction.

We have followed your suggestion and included the chapter in the introduction.

Lines 136-138: If it is not that important (I guess it is not since it is not shown) it shouldn't be mentioned at all.

We now include the Bz plot in Figure 1 as Bz is an important parameter in determining whether pulsations are produced by internal or external processes.

Line 152: Define cone angle. Also I don't see it anywhere in the figure. Instead I see the three components of speed which are not discussed at all. Figures are already too many (16!!!). Since Kp and speed are not discussed at all remove them and merge figures 1 and 2 (or even better provide the total solar wind speed only).

We followed your advice. We defined the cone angle and included it and the total solar wind speed in Figure 1. We merged Figures 1 and 2. Now there are 14 figures in the paper. We discussed the solar wind speed in the section on testing generation mechanisms.

Lines 170-178: The authors discuss the time-lag between solar wind pressure and compressions at GEO. Is this really important for the conclusions of this work? More-over, I'm left with the feeling that the use of GOES measurements, in general, do not provide any significant observational evidence in this work. If I'm wrong then I believe that it should be discussed more clearly but if I'm not the authors should consider not using it at all.

The GOES data provide important spatial context for understanding this event. In particular, they help to contrast some of the features of the Pc4 and Pc5 waves observed at all four spacecraft. GOES data also confirm the value of data at geosynchronous orbit for monitoring solar wind conditions and the importance of solar wind pressure enhancements for stimulating and even amplifying compressional waves in the dayside magnetosphere. However, because of the much more complete instrumentation available on the Van Allen Probes, the remainder of this paper will focus on the observations from the latter spacecraft.

Lines 187-189: The authors state "Prior to the arrival of the strong solar wind dynamic pressure variations, RBSP-A observed very weak compressional pulsations with Pc5 periods and amplitudes of 1-3 nT from 18:15 to 18:55 UT." This is not shown anywhere.

The weak compressional pulsations observed by RBSP-A are not visible in Figure 3 because of the very large scale in this figure but readers can see some traces of them in Figure 7.

In figures 5 and 6 the authors show the magnetic field in GSM coordinates along with the total magnetic field yet they are referring to compressional pulsations. If the authors mean the Btot they should mention it along with the assumption that Btot is almost the same with Bcomp. Nevertheless, since they are showing the MFA coordinates later in the text, I don't understand

the usage of these two figures especially when they also contain the x,y,z coordinates which are not discussed at all.

We changed the text and Figures 4 and 5. Figure 5 shows only data in mean field-aligned coordinates, not including the field magnitude, and only for a shorter time interval. We discuss the pulsations in FAC and comment on the phase relations between the 3 components.

Lines 208-211: Please rename X-Y-Z to Poloidal-Toroidal-Compressional.

The definitions of the field-aligned coordinates that we used are precise, and are strictly based on observations. In the real rather than ideal magnetosphere, ULF waves, whether toroidal, poloidal, or compressional, often have at least some power in 2 or more components in a field-aligned system. Thus we do not label the three components of the magnetic field toroidal, poloidal, and compressional. Nevertheless, Pc5 pulsations are called compressional because of the prominent Bz component.

lines 271-274: The oscillations are of course visible but the rest of the statements are not supported by this plot as the reader can understand nor the exact frequency of these waves neither the phase difference. Maybe a simple filtering would give prominence to these pulsations or even better a spectral analysis.

We changed Figure 10 (formerly Figure 12) to show that that the intensities of electrons with energies from tens of keV to 2 MeV oscillate with Pc5 periods corresponding to those of the magnetic field. The energetic electron fluxes oscillated out of phase with the compressional Bz component of Pc5 magnetic field pulsations and did not display any phase differences across all energies (see an expanded view for some selected energies, Figure 10b). We calculated the dynamic spectra for electrons at all available energies observed by RBSP-A and -B and found pulsations with frequencies similar to those for the compressional Pc5 pulsations (see Figure A of this reply below). The lower energy electron fluxes displayed more noticeable enhancements as a response to the compressions of the magnetosphere.

Line 279: What is P and B? Please define.

We corrected the sentence: . . .the antiphase relation between the plasma and magnetic field pressures suggests that particle pitch angle distributions peak near 90◦.

Figure 13: There is a completely different behavior between low and high energy PA distributions yet the authors do not discuss it at all. I think there is much more information in this figure which should be further discussed.

We are not sure what feature in the figure the referee is addressing. We wish only to note: (1) the fact that pitch angle distributions peak near 90◦ pitch angles, (2) there are successive enhancements in response to compressions of the magnetosphere (for example at 19:40 and 20:05 UT at RBSP-A), and (3) these enhancements are most pronounced at the lower energies. At higher energies, flux variations associated with the radial gradients dominate the instrument response, as indeed can also be seen in Figure 10a.

Line 289: Please rephrase.

We slightly rephrased the sentence: The compressional components oscillated with a frequency twice that of the transverse component.

Lines 310-311: I don't understand this sentence. What do the authors mean by "most prominent". In figure 9, the double frequency is very pronounced from â´Lij19:54 until after 20:32.

The referee's reading of Figure 9 (now Figure 7) is correct, but this sentence refers to Figure 12, which presents the same data in a different format that does not include the relatively broad time window feature that is intrinsic to dynamic Fourier spectra. To prevent future confusion, we have added the following words at the end of this sentence: "in these line plots."

Lines 350-353: I would like to see the filtered time series of pressure or its fourier transform. As Kepko et al., 2002 have shown, the time interval that the authors examine is the ideal one for pulsations originating in the solar wind pressure.

We stated:

First, with the exception of the interval from 19:35 UT to 19:55 UT, the Wind observations shown in Figure 1 provide no evidence for periodic solar wind drivers in the Pc5 range, be they density variations or IMF fluctuations, thus ruling out solar wind pressure pulses as the direct cause of the Pc4-5 pulsations. In what follows we show WIND data time-shifted 53 minutes (consistent with Figure 3), and confirm that solar wind pressure oscillations are not the direct cause of the Pc4-5 pulsations. Figure B of this reply compares dynamic spectra of the WIND solar wind pressure (shifted by 53 min) and of the RBSP-A total magnetic field from 17:30 UT to 22:00 UT on January 1, 2016. There is no evidence for significant solar wind pressure pulsations during this 4.5 hour interval. Only three very weak intensifications of pressure pulsation activity at Wind were observed during short intervals but they began 1.5 hour later than the generation of the magnetic Pc5 pulsations. Figure C presents Wind time-shifted filtered data in the band of frequencies from 2 to 10 mHz. A monochromatic wave packet with frequency of ~5 mHz only appeared between ~20:30 and ~20:50 UT that we marked in the Wind observations (not time-shifted) presented in Figure 1. We thus rule out solar wind pressure pulses as the direct cause of the Pc4-5 pulsations.

Line 369: Please rephrase.

We rephrased this sentence. As Figures 10 (a, b) demonstrate, RBSP-A shows no evidence in the electron observations for any such phase reversal at any relevant energies.

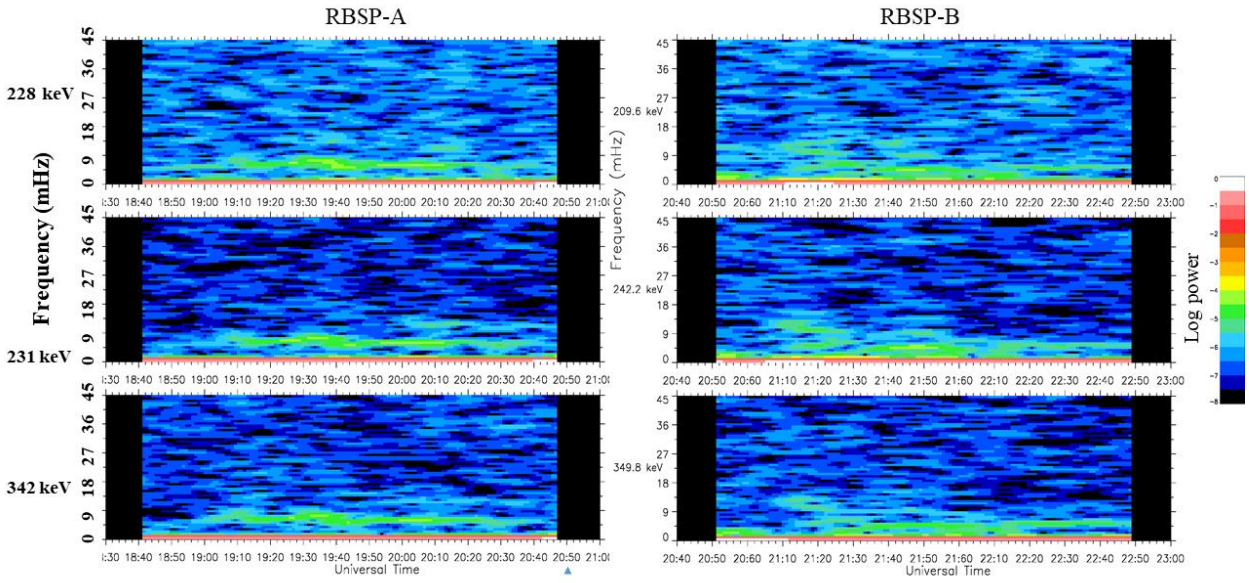

Figure A. Dynamic spectra for electrons with selected energies observed by RBSP-A from 18:30 to 21:00 UT and by -B from 20:40 to 23:00 UT on January 1, 2016

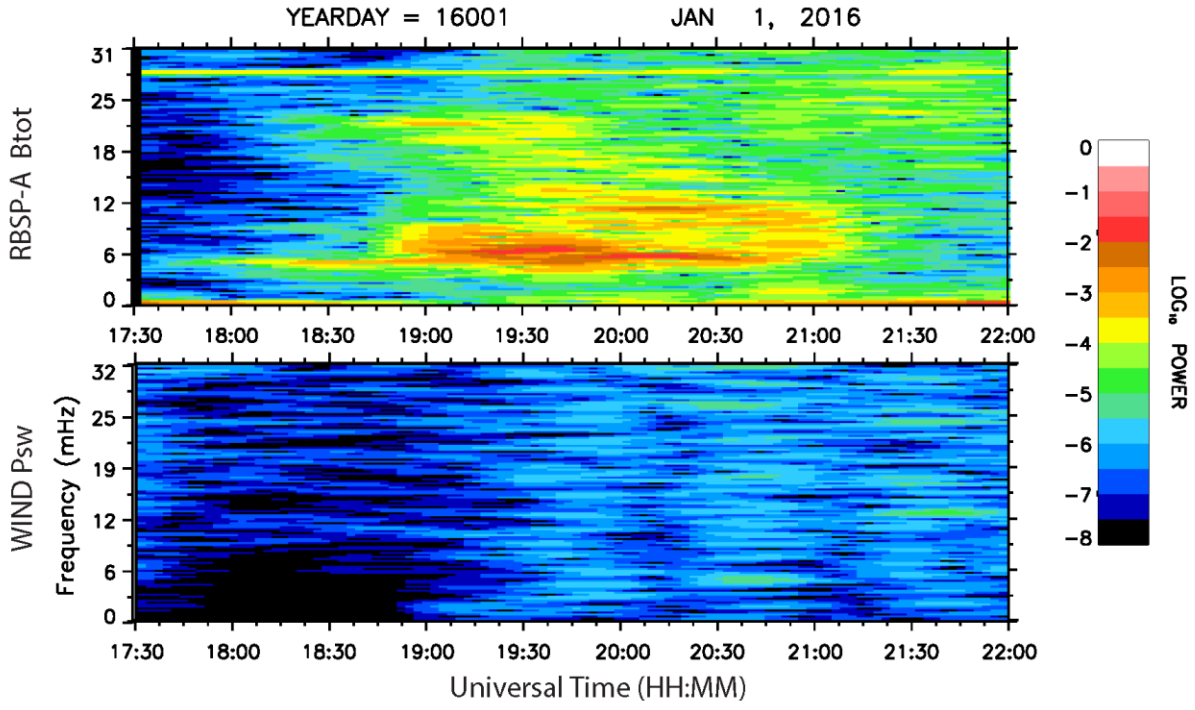

Figure B. Dynamic spectra of the RBSP-A total magnetic field strength and the WIND solar wind pressure from 17:30 UT to 22:00 UT on January 1, 2016.

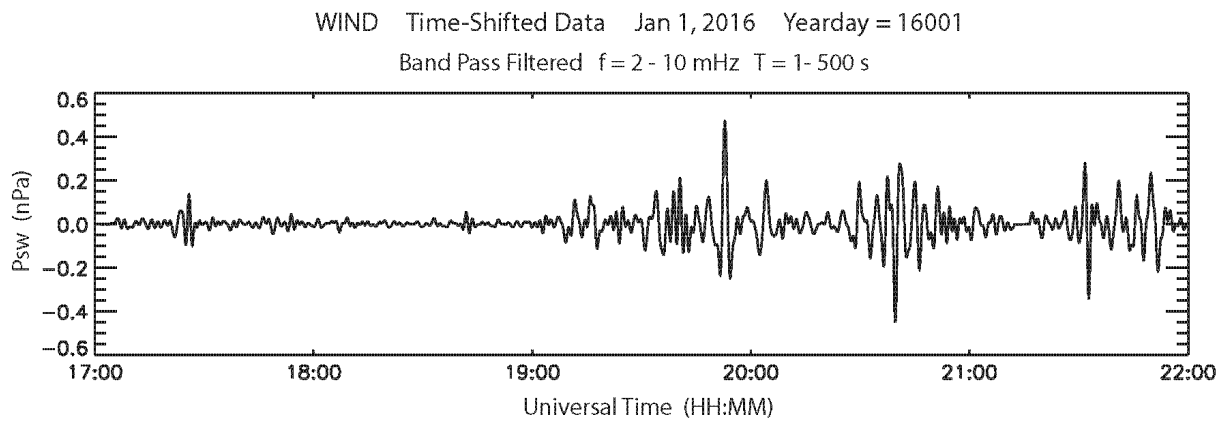

Figure C. **Wind time-shifted filtered data in the band of frequencies from 2 to 10 mHz from 17:00 UT to 22:00 UT on January 1, 2016.**

Dear Referee #2,

Thank you very much for your comments and corrections. We have adopted all them. Enclosed, please find our replies to your remarks.

Line 58: "They have several Re wavelengths". Suggest "The have wavelengths of several **R_E" –**

We corrected the sentence: They have wavelengths of several Earth radii.

Line 108: please define what you mean by "mode of the waves" and "nodal structure". Are we referring to azimuthal mode structure and latitudinal node structure? Or does "mode" refer to, e.g., compressional vs transverse waves? –

We changed the sentence as follows:

We investigate the type of pulsation (compressional versus transverse), their harmonic mode, and their latitudinal nodal structure.

Line 138: since solar wind observations have not yet been introduced as a figure, suggest removing the words "(not shown)".

We now show the solar wind observations in the final version of the paper.

Lines 163 et seq, and Figure 4. Please describe how the solar wind values are lagged. Is this a simple ballistic propagation estimation, a best fit estimation, or are propagation techniques such as those used in producing OMNI solar wind data used? –

To determine the lag time between the Wind and GOES-15 observations we related individual magnetosphere compressions to corresponding dynamic pressure variations.

The good correspondence of GOES magnetic field enhancements to solar wind dynamic pressure pulses at the beginning and the end of the interval facilitated this task. Additionally, we confirmed these empirically derived lag times with simple ballistic estimates based on the solar wind velocity and the distance of Wind from Earth. Finally, we confirmed our estimates by examining the OMNI parameters.

Line 234: "min" -> "minute" –

We changed min to minute

Line 282: remove spurious period (".") between words "distribution" and "peak".

We removed period between words distribution and peak.

The figure confirms that pitch angle distributions

Line 359: "Therefore, we conclude like many previous researchers that the...". Please provide citations for previous conclusions, or remove words "like many previous researchers". –

We changed the sentence: Therefore, we conclude that the compressional Pc5 pulsations were excited by processes internal to the magnetosphere.

Lines 379 et seq. HOPE, EMFISIS, and RBSPICE contributions should be noted and described in Section 2, "Resources".

We added additional descriptions of the RBSP instruments.

This paper employs observations of the most abundant ion components as well as electrons, over the 0.001–50 keV energy range of the core plasma populations from the HOPE instrument, populations of 20-4000 keV ion and electrons from the MagEIS instrument [Blake et al., 2013] in the Energetic Particle, Composition, and Thermal (ECT) suite [Spence et al., 2013], fluxes of ions over the energy range from ~20 keV to ~1 MeV and electrons over the energy range ~25 keV to ~1 MeV (RBSPICE) [Mitchell et al., 2013] in conjunction with observations from the magnetometer in the Electric and Magnetic Field Instrument Suite and Integrated Science suite (EMFISIS) [Kletzing et al., 2013], and the Electric Field and Waves (EFW) [Wygant et al., 2013] instrument. We examine electric and magnetic field measurements with 11 s and 4 s time resolution, respectively, and differential particle flux observations with ~11 s (spin period) time resolution.

Thank you again for your help,

Regards,

Galina Korotova.

Multipoint Observations of Compressional Pc5 Pulsations in the Dayside Magnetosphere and Corresponding Particle Signatures

Galina Korotova[1,2], David Sibeck[3], Mark Engebretson[4], Michael Balikhin[5], Scott Thaller[6], Craig Kletzing[7], Harlan Spence[8], and Robert Redmon[9]

[1]IPST, University of Maryland, College Park, MD, USA

[2]IZMIRAN, Russian Academy of Sciences, Moscow, Troitsk, Russia

[3]NASA/GSFC, Code 674, Greenbelt, MD, USA

[4] Department of Physics, Augsburg University, Minneapolis, MN, USA

[5]Department of Automatic Control and Systems Engineering, University of Sheffield, Sheffield, UK.

[6] LASP, University of Colorado, Boulder, CO, USA

[7]Department of Physics and Astronomy, Iowa University, Iowa City, IA, USA

[8]EOS, University of New Hampshire, Durham, NH, USA

[9]Solar and Terrestrial Physics division, NGDC/NOAA, Boulder, CO, USA

Abstract

We use Van Allen Probes Radiation Belt Storm Probes-A and -B (henceforth RBSP-A and -B) and GOES-13 and -15 (henceforth G-13 and G-15) multipoint magnetic field, electric field, plasma, and energetic particle observations to study the spatial, temporal, and spectral characteristics of compressional Pc5 pulsations observed during the recovery phase of a strong

geomagnetic storm on January 1, 2016. From ~19:00 UT to 23:02 UT, successive magnetospheric compressions enhanced the peak-to-peak amplitudes of Pc5 waves with 4.5-6.0 mHz frequencies from 0-2 to 10-15 nT at both RBSP-A and -B, particularly in the prenoon magnetosphere. Poloidal Pc4 pulsations with frequencies of ~22-29 mHz were present in the radial Bx component. The frequencies of these Pc4 pulsations diminished with increasing radial distance, as expected for resonant Alfvén waves standing along field lines. The GOES spacecraft observed Pc5 pulsations with similar frequencies to those seen by the RBSP, but Pc4 pulsations with lower frequencies.

Both RBSP-A and -B observed frequency doubling in the compressional component of the magnetic field during the Pc5 waves, indicating a meridional sloshing of the equatorial node over a combined range in Z_{SM} from 0.25 to -0.08 Re, suggesting that the amplitude of this meridional oscillation was ~0.16 Re about an equatorial node whose mean position was near Z_{SM} = ~0.08 Re. RBSP-A and -B HOPE and MagEIS observations provide the first evidence for a corresponding frequency doubling in the plasma density and the flux of energetic electron, respectively. Energetic electron fluxes oscillated out of phase with the magnetic field strength with no phase shift at any energy. In the absence of any significant solar wind trigger or phase shift with energy, we interpret the compressional Pc5 pulsations in terms of the mirror mode instability.

Introduction

ULF pulsations with periods of 100 s or greater and high azimuthal wave numbers (m) with magnetic field perturbations in the radial direction and electric field perturbations in the azimuthal direction within the Earth's magnetosphere are typically poloidal waves [Sugiura and Wilson, 1964]. According to Elkington et al. [2003], energetic particles with drift frequencies of 6.7-22 mHz and 1.7-6.7 mHz can readily interact with corresponding high-m poloidal Pc4 and Pc5 pulsations. Because the atmosphere and ionosphere screen these high-m waves from the ground, they can only be studied with the help of satellite observations. Past studies of Pc4 and Pc5 pulsations with significant compressional components employed observations from locations at or near geosynchronous orbit [e.g., Dai et al., 2013]. Higbie et al. [1982] and Nagano and Araki [1983] showed that long-lasting compressional Pc5 pulsations occur most frequently in the dayside magnetosphere during the recovery phase of magnetic storms. Storm-time Pc5

pulsations occur in the afternoon sector between 12:00 and 18:00 local time following injections of ring current particles [Kokubun, 1985].

A number of studies have examined compressional Pc5 waves outside geostationary orbit. According to these studies, compressional Pc5 waves were observed in the dawn [Hedgecock, 1976], dusk [Constantinescu et al., 2009] and noon [Takahashi et al., 1985] sectors. Zhu and Kivelson [1991] reported that intense compressional waves are a persistent feature on both flanks of the magnetosphere. Compressional Pc5 pulsations occur within ~20° latitude of the magnetic equator [Vaivads et al., 2001]. **They have wavelengths of several radii** [Walker et al., 1982] and often exhibit harmonics. Elkington et al. [2003] noted that poloidal and compressional modes are far more effective for the radial transport of energetic particles than the toroidal mode. Two methods are used to identify the harmonic mode of a poloidal oscillation. The first compares the phase difference between the radial component of the magnetic field and the azimuthal component of the electric field [Takahashi et al., 2011]. The second compares observed wave frequencies with the eigenfrequencies predicted by theory [Cummings, 1969]. The multi-satellite study of Takahashi et al. [1987a] showed that a compressional Pc 5 wave had an antisymmetric standing structure.

Compressional Pc5 pulsations have been ascribed to numerous excitation mechanisms. They can be produced by internal and external processes. It is supposed that the solar wind is the main external source for pulsations produced by the Kelvin-Helmholtz (KH) instability at the magnetopause or the inner edge of the low-latitude boundary layer [e.g., Guo et al., 2010]. Observations indicating enhanced rates of Pc5 occurrence during periods of greater solar wind velocity support this model [e.g., Engebretson et al., 1998]. Transient variations in the dynamic pressure of the solar wind or foreshock [e.g., Wang et al., 2018; Shen et al., 2018] that cause abrupt changes in the magnetic field strength in the magnetosphere and sudden impulses in the ionosphere [e.g., Zhang et al., 2010, Sarris et al., 2010] provide another possible trigger for Pc5 pulsations. External pressure impulses can cause compressional oscillations of the magnetosphere with discrete eigenfrequencies, known as global modes or cavity/waveguide modes [Samson et al., 1992]. Periodic solar wind dynamic pressure variations directly drive some compressional magnetospheric magnetic field oscillations [e. g., Kepko et al., 2003; Motoba et

al., 2003]. Takahashi and Ukhorskiy [2008] considered solar wind pressure variations as the main external driver of Pc5 pulsations observed at geosynchronous orbit in the dayside magnetosphere.

Internal generation mechanisms for compressional Pc5 pulsations include the drift-bounce resonant instability which occurs for particles with resonance drift and bounce periods [Southwood et al., 1969] and the drift-mirror instability in the presence of strong temperature anisotropies [Chen and Hasegawa, 1991]. In high β plasmas (β is the plasma pressure divided by the magnetic pressure), these mechanisms favor antisymmetric waves [Cheng and Lin, 1987].

One possible generation mechanism for compressional Pc5 pulsations at geosynchronous orbit is a drift-mirror instability of ring current particles [e.g., Lanzerotti et al., 1969]. While the observed anticorrelated magnetic field strength and ion flux oscillations are expected for a drift mirror wave [Kremser et al., 1981], the instability criterion is generally not satisfied [Pokhotelov et al., 1986]. One possible reason for the lack of consistency between theory and observation might be because the real geometry of the magnetosphere is not taken into account [Cheng and Lin, 1987]. Compressional pulsations are often accompanied by pulsations in particle fluxes [Kremser et al., 1981; Liu at al., 2016]. Particle observations can provide useful information on the spatial and wave structure of ULF pulsations. Lin et al. [1976] explained flux oscillations as the adiabatic motion of particles in a magnetohydrodynamic wave. Kivelson and Southwood [1985] studied charged particle behavior in compressional ULF waves and showed that "a mirror effect" is the dominant cause for particle flux modulations. Finite gyroradius effects enable detection of gradients in particle flux associated with waves [e.g., Korotova et al., 2013].

We use multipoint magnetic field, plasma, and energetic particle observations from RBSP-A and -B and G-13 and -15 to study the spatial, temporal, and spectral characteristics of compressional Pc5 pulsations observed deep within the magnetosphere during the recovery phase of the strong magnetic storm which began on December 31, 2015. **We investigate the type of pulsation (compressional versus transverse), their harmonic mode, and their latitudinal nodal structure.** We focus on the properties of double frequency pulsations that occurred in the vicinity of the geomagnetic equator. We demonstrate that the energetic particles respond

directly to the compressional Pc5 pulsations and also exhibit a double frequency oscillation. We search for possible solar wind triggers and test two possible generation mechanisms: drift-bounce resonance, and mirror instability. The paper is organized as follows: Section 2 describes instruments and resources. Section 3 presents the solar wind and IMF conditions. Section 4 provides an analysis of these waves and their generation mechanisms.

2. Resources

The Van Allen Probes mission can be used to study the geospace response to a fluctuating solar wind. The mission began in August 2012 with a twin spacecraft launch into similar 10° inclination orbits with perigee altitudes slightly greater than 600 km and apogee altitudes just beyond 30000 km [Mauk et al., 2012]. The spacecraft carry instruments that measure electromagnetic fields, waves, and charged particle populations deep within the magnetosphere. **This paper employs observations of the most abundant ion components as well as electrons, over the 0.001–50 keV energy range of the core plasma populations from the HOPE instrument, populations of 20-4000 keV ion and electrons from the MagEIS instrument [Blake et al., 2013] in the Energetic Particle, Composition, and Thermal (ECT) suite [Spence et al., 2013], fluxes of ions over the energy range from ~20 keV to ~1 MeV and electrons over the energy range ~25 keV to ~1 MeV (RBSPICE) [Mitchell et al., 2013] in conjunction with observations from the magnetometer in the Electric and Magnetic Field Instrument Suite and Integrated Science suite (EMFISIS) [Kletzing et al., 2013],** and the Electric Field and Waves (EFW) [Wygant et al., 2013] instrument. We examine electric and magnetic field measurements with 11 s and 4 s time resolution, respectively, and differential particle flux observations with ~11 s (spin period) time resolution. .The data are provided by NASA/GSFC's CDAWEB in the MGSE (modified GSE) coordinate system. We use magnetic field data from G-13 and -15 with 0.5 s time resolution [Singer et al., 1996]. Finally, we employ Wind solar wind magnetic field and 3DP plasma data with 3 s time resolution [Lepping et al., 1995; Lin et al., 1995].

3. Orbits and solar wind and geomagnetic conditions

Figure 1 presents the Bz component of the interplanetary magnetic field observed at Wind, and geomagnetic activity Dst and AE indices obtained from the OMNI database (upper panels) from 12:00 UT on December 30 to 00:00 UT on January 2, 2016. The bottom panels show Wind observations of the magnetic field components, total magnetic field strength, cone angle, pressure, plasma density, and velocity from 16:00 UT on January 1, 2016 to 00:00 UT on January 2. 2016 during which time the spacecraft moved from GSM (X, Y, Z) = (194.7, 20.1, -12.5) Re to (194.8, 23.6, -7.4) Re. The pulsation events to be studied here occurred late on January 1, 2016, following a prolonged period of strongly southward IMF orientation and geomagnetic activity. A substantial increase in the solar wind dynamic pressure early on December 31 was followed by a strong southward IMF that persisted from 19:00 UT on December 31, 2015 until 09:00 UT on January 1, 2016. A strong electrojet with AE index greater than 2100 nT at 12:36 UT on December 31, 2015 was followed by two moderate substorms that enhanced AE at ~14:00 and 18:45 UT on January 1, 2016. The Dst index responded by reaching a value as low as -110 nT at 00:30 UT on January 1, 2016**.** Shading highlights the interval from ~19:00 to 23:02 UT late in the recovery phase and late in the day on January 1, 2016 when the Van Allen Probes and GOES spacecraft observed the strong compressional Pc5 pulsations of interest to this study**.**

The latter interval (bottom panels) was marked by strong variations in the solar wind dynamic pressure. Shading marks an interval of depressed magnetic field strengths and generally anticorrelated enhanced densities, velocities and solar wind dynamic pressures. T**he cone angle, θ, defined as the angle between the IMF and the Sun-Earth line was less than 45^0 during this interval.** The magnetic field was briefly aligned with the Sun-Earth line (Bx) at the center of the interval from 20:00-21:00 UT. For most of the ~4h long shaded interval, IMF Bx (By) was predominantly positive (negative) and the Bz component remained almost constant near 0 nT, indicating a spiral and equatorial IMF configuration. The total magnetic field strength decreased from 7.9 nT at 18:00 UT to 2.2 nT at 19:48 UT **and the solar wind velocity and dynamic pressure increased from 426 km/s** and 0.62 nPa at 18:00 UT to 457 km/s and to 3.37 nPa at 20:47 UT, respectively. At ~ 22:20 UT almost all parameters returned to their initial undisturbed values.

Figure 2 presents RBSP-A and -B and G-13 (MLT~ UT-5) and -15 (MLT~ UT- 9) trajectories from 15:00 UT to 24:00 UT on January 1, 2016 in the X-Y and X-Z GSM planes. Open circles mark the beginning of the spacecraft trajectories which are duskward for the GOES spacecraft and duskward at apogee for the Van Allen Probes. All of the spacecraft were north of the equator when in the dayside magnetosphere. The thick line segments (dots) indicate the locations of the spacecraft at the times when (weak) Pc5 magnetic field pulsations occurred.

Figure 3 compares lagged Wind solar wind dynamic pressure variations with G-13 and -15 observations of the dayside magnetospheric magnetic field. The arrows connect enhancements of the solar wind dynamic pressure to corresponding compressions of the magnetosphere. **To determine the lag time between the Wind and GOES-15 observations we related individual magnetosphere compressions to corresponding dynamic pressure variations. Additionally, we confirmed these empirically derived lag times with simple ballistic estimates based on the solar wind velocity and the distance of Wind from Earth.** It is relatively easy to associate the GOES magnetic field enhancements with corresponding features in the solar wind dynamic pressure at the beginning and the end of the interval but less easy from 19:50 UT to 21:20 UT corresponding to ~ 20:45 UT and 22:15 UT at the GOES spacecraft. The lag time from Wind to the Earth is not uniform and depends on IMF orientation. At the beginning and end of the interval, when the IMF was spiral (Bx >0, By <0), the lag was in the range of ~46 to 58 min. Consistent with expectations, the lag became greater for the interval from ~ 19:50 UT to 21:20 when the IMF was nearly radial (By and Bz ~0 nT). The reasonable correspondence of the magnetosphere compressions to solar wind dynamic pressure variations demonstrates that Wind was a good monitor for solar wind conditions and that a series of pressure enhancements were applied to the magnetosphere during the interval of interest. Pc5 pulsation amplitudes at G-13 and -15 were greater during the interval of enhanced solar wind dynamic pressure and magnetospheric magnetic field strengths than they were at earlier and later times.

4. Pulsation Observations

4.1. Spatial characteristics of Pc5 pulsations

Consider the spatial extent, temporal, and spectral characteristics of the compressional Pc5 pulsations. **Figure 4a shows G-13 and -15 observations of the total magnetic field strength from 18:00 UT to 24:00 UT. The spacecraft observed long-duration Pc5 pulsations over a wide longitudinal region in the pre- and post-noon magnetosphere from 10:00 to 15:20 MLT (Figure 2). G-15 observed weak, less than ~5 nT amplitude, Pc5 waves from 18:28 UT to 19:04 UT prior to the main event. During the main event from 19:04 to 23:00 UT, the magnetosphere was compressed (Figure 3), magnetic field strengths increased and the amplitude of these waves increased to values ranging from 10 to 16 nT with peak amplitudes prior to local noon. G-13 observed weak Pc5 pulsations with amplitudes of 2-4 nT throughout most of the time interval from 16:40 UT (not shown) to 21:00 UT. During the interval from 19:34 UT (~14:45 MLT) to 20:10 UT (~15:20 MLT), the pulsations reached slightly stronger amplitudes of 5-8 nT. At 23:02 UT all Pc5 wave activity at both GOES stopped.**

Figure 4b shows the RBSP-A and -B total magnetic field strength from 18:40 UT to 21:10 UT and from 20:40 UT to 23:10 UT, respectively, on January 1, 2016. Taken together, RBSP-A and -B observed Pc5 pulsations that occupied the inner dayside magnetosphere from 5.26 to 5.75 R_E and from 09:56 to 12:44 MLT (Figure 2). Prior to the arrival of the strong solar wind dynamic pressure variations from 18:15 to 18:55 UT RBSP-A observed very weak pulsations with Pc5 periods and amplitudes of 1-3 nT (not visible at this scale). After the compression of the magnetosphere just after 19:00 UT, the pulsation amplitude at RBSP-A increased to values ranging from 10 to 15 nT with the peak amplitude occurring prior to local noon (Figure 4b). RBSP-B observed similar compressional Pc5 pulsations from 20:46 UT that ceased simultaneously with the end of the magnetospheric compression at about 23:02 UT.

To determine the type of the Pc5 waves we converted the magnetic field observations from GSE into field-aligned coordinates (FAC). Here the Z axis lies parallel to the locally-averaged magnetic field. The Y axis points approximately azimuthally eastward and is transverse to B and to the outward radius vector. The X axis completes the right-handed system and is directed approximately radially outward from Earth. **Figure 5 presents RBSP-A and -B magnetic field observations in FAC. The Bz component is the value of the total magnetic field after subtraction of a 16-minute sliding average**. The Pc5 pulsations are observed in all three components but the

amplitudes of the azimuthal By and radial Bx components are rather small and do not exceed 7 nT. The compressional Bz component is much more pronounced for both spacecraft, reaching amplitudes of 14-15 nT before local noon. Consequently, the pulsations are primarily compressional. The Bz component oscillated out of phase with the Bx component at RBSP-A and in phase at RBSP-B and in quadrature with the By component. Simultaneous RBSP-A and -B electric and magnetic field measurements provide an opportunity to study the mode of the Pc5 waves. Determining the harmonic mode of the Pc5 waves requires us to consider the phase of the azimuthal component of the electric field Ey with respect to the radial component of the magnetic field Bx as a function of latitude [Takahashi et al., 2011]. Figure 6 shows that the phase of the Ey component leads that of the Bx component by 90° at RBSP-A from 19:10 UT to 20:00 UT and therefore the Pc5 waves are second harmonic in nature.

4.2. Spectral characteristics

We calculated dynamic spectra for the magnetic field pulsations. Figure 7 presents the radial, azimuthal and compressional components of the dynamic spectra of the magnetic field at RBSP-A and -B from 18:00 to 21:10 UT and from 20:00 UT to 23:10 UT on January 1, 2016, respectively. The color bar on the right shows the scale for power for frequencies ranging from 0 to 41 mHz in each component. The magnetic field exhibited several wide-band enhancements at frequencies ranging from 4 to 29 mHz. As expected for compressional Pc5 pulsations, both GOES spacecraft observed the strongest power densities in the Bz component at dominant frequencies of ~4.5-6 mHz. Red arrows in the Bz panels of Figure 7 for RBSP-A and -B indicate the double frequency pulsations at ~5.5 mHz and ~11 mHz. We calculated Fourier spectra for the three components of the RBSP-A and -B magnetic field in 600 second sliding-averaged mean FAC for each thirty minute interval during the event. Figure 8 presents examples of Fourier spectra calculated for the RBSP-A and -B magnetic field from 19:30 UT to 20:00 UT and from 22:30 UT to 23:00 UT, respectively, on January 1, 2016. The red arrows show the dominant frequencies at 5.5 and 5 mHz observed at the two spacecraft, corresponding to periods of 170-200 s. RBSP-A and -B were situated three hours in local time apart; the similar frequencies

indicate that conditions in the dayside magnetosphere remained steady for a long time and over a broad region.

In passing, we note the presence of Pc4 pulsations. Returning to Figure 7, we see enhanced power densities at frequencies of ~22-29 mHz with dominant frequencies from 23 to 27 mHz primarily in the radial Bx component. These can be ascribed to poloidal Pc4 produced simultaneously with the Pc5 but likely with another energy source. The frequencies of the Pc4 pulsations decrease with increasing radial distance, as expected for resonant standing Alfvén waves [Sugiura and Wilson, 1964]. Pulsation periods depend upon the magnetic field line length, the magnetic field magnitude, and the ion density**.** Shorter field line lengths and enhanced magnetic field strengths closer to Earth decrease pulsation periods. Blue arrows in Figure 8 indicate Pc4 pulsations at ~25-27 mHz.

Figure 9 presents dynamic spectra for the G-13 and -15 magnetic field in FAC from 18:00 UT to 24:00 UT on January 1, 2016. Spectral power was calculated for frequencies from 0 to 48 mHz. Like the RBSP-A and -B magnetic field spectra, there are two broad frequency band enhancements corresponding to Pc4 and 5 frequencies. The dominant frequencies for the compressional Pc5 pulsations occur from 4.5 to 6.5 mHz. These frequencies are similar to those observed by Van Allen Probes and we suppose that they were generated by the same sources. The Pc4 pulsations are most pronounced in the radial Bx component and display strongest spectral power densities in the frequency range from 13 to 21 mHz. These frequencies are lower than those observed by Van Allen Probes, since the GOES spacecraft were located further radially outward from Earth [Sugiura and Wilson, 1964]. The frequencies of the long-lasting Pc4 pulsations observed by G-15 depended on local time. They decreased from 20-22 mHz in the prenoon magnetosphere to 14-17 mHz near local noon, perhaps in response to differing conditions (e.g., densities). Takahashi at el. [1984] noted that an increase in plasma mass density from morning to afternoon is typical at geosynchronous orbit. Since the frequencies of the Pc4 pulsations depended on local time and radial distance from Earth, their sources must be more localized than those for the Pc5 pulsations.

4.3. Particle signatures

Energetic particle observations provide further information concerning this event. We inspected RBSP-A and-B MagEIS observations of energetic particles from 18:30 UT to 21:00 UT and from 20:40 UT to 23:10 UT on January 1, 2016, respectively, and found that the intensities of electrons with energies from tens of keV to 2 MeV oscillated with Pc5 periods corresponding to those of the magnetic field. **Figures 10a and b show an example of RBSP-A observations of electron fluxes (a) in the energy range of from 31.5 keV to 1704 keV from 18:30 UT to 21:00 UT and (b) their expanded view for selected energies from 19:20 UT to 20:00 UT. The energetic electron fluxes oscillated out of phase with the compressional Bz component of Pc5 magnetic field pulsations and did not display any phase differences across all energies.** The depth of modulation (the peak to valley ratio) is larger for higher energy electrons consistent with the results of Liu et al. [2016] who interpreted similar observations in terms of mirror mode waves. The lower energy electron fluxes displayed more noticeable enhancements as a response to the compressions of the magnetosphere. Kivelson and Southwood [1985] noted that the maintenance of pressure balance in low- frequency compressional waves usually requires the presence of some pitch angle anisotropy **and the antiphase relation between the plasma and magnetic field pressures suggests that particle pitch angle distributions peak near 90°.** Figure 11 presents RBSP-A and -B observations of pitch angle distributions for electrons with energies from 54 keV to 1060 keV from 18:30 to 21:00 UT and from 20:40 UT to 23:10 UT on January 1, 2016, respectively. The figure confirms that pitch angle distributions peak near 90°. Furthermore, it shows that the electron intensities display quasi-periodic enhancements at all energies with the strongest at pitch angles near 90°.

4.4. Double-frequency pulsations

When RBSP-A and -B were in the vicinity of the geomagnetic equator the compressional Pc5 pulsations displayed peculiar features indicating frequency doubling. The compressional components oscillated with a frequency twice that of the transverse component. Coleman [1970] was the first to report observations of such events in the geosynchronous magnetic field.

Higuchi et al. [1986] called them harmonic structures when the first and second harmonics exhibited similar amplitudes and transitional structures when the amplitudes of the alternating peak were different. Takahashi [1987b] interpreted double-frequency oscillations in terms of a model invoking the second harmonic structure of an antisymmetric standing wave in which the location of the equatorial node of field-lined displacement oscillates in phase with the wave. Cheng and Qian [1994] presented a model for the magnetic field perturbations during the pulsations reported by Takahashi et al. [1987a, 1990]. Figure 6 in the paper of Korotova et al. [2013] illustrates how low-latitude spacecraft can observe two magnetic field strength enhancements per wave cycle when the equatorial node oscillates latitudinally up and down in phase with an antisymmetric compressional wave. Right at the equator the spacecraft observes identical amplitudes for the two compressions. At any other latitude the two compressions at the spacecraft will have different magnitudes and the imbalance between them increases when the spacecraft moves farther from the equator. Takahashi et al. [1997b] showed that that a latitudinal shift of a fraction of degree can turn a harmonic Bz structure into a nonharmonic structure. Spacecraft located far from the magnetic equator do not observe frequency doubling, just a single enhancement. Korotova et al. [2013] derived the latitudinal structure of the waves by invoking north-south sloshings of the low-latitude node.

Figures 12a and b present (a) RBSP-A and -B observations of double frequency magnetic pulsations and (b) their locations in the X-Y GSM and X-Z SM planes. Dashed lines in Figure 12a indicate intervals when the double frequency pulsations in Bz are most prominent: 20:45-20:54 UT at RBSP-A and 21:03 UT to 21:31 UT at RBSP-B **in these line plots.** However, the amplitudes of the second harmonic are generally much lower than those of the first harmonic. At these times, e.g. from 20:05 to 20:45 UT at RBSP-A and 21:35-21:55 UT at RBSP-B, the second harmonic compressions in Bz are barely perceptible in these line plots. Model predictions for the magnetic field perturbations associated with an equatorial node whose latitude oscillates in phase with an antisymmetric poloidal wave indicate that the ratio of the amplitudes of the first to second harmonic compressions should change with latitude, being ~1 at the average position of the low-latitude node and ~0 at and beyond the maximum latitude to which the oscillating node can reach [Takahashi et al., 1987b]. To determine the meridional motion of the magnetic field node we

measured amplitudes of the first and second harmonics of the compressional pulsations. We found that RBSP-A observed ratios near 1 at Z_{SM} = ~0.08 Re while RBSP-B observed ratios near 1 at Z_{SM} = ~0.10 Re. These are the locations where the southward-moving spacecraft pass through the mean positions of the equatorial node. Figure 12a shows that RBSP-A observed second harmonics from Z_{SM} = 0.25 to 0.04 Re, while RBSP-B observed them from Z_{SM} = 0.19 to -0.08 Re. Consequently, we believe that the equatorial node oscillated with an amplitude of at least 0.15 to 0.18 Re. Note however, that the ratio of the first to second harmonics does not show a smooth transition as the spacecraft move equatorward. Either the amplitude of the compressional pulsation or the meridional oscillation in the equatorial node varied in time, probably abruptly.

Figures 10a and b show that the compressional pulsations modulated energetic electrons observed by RBSP-A and we should therefore expect to find the signatures of the double-frequency pulsations not only in the magnetic field but also in the fluxes of particles. Takahashi et al. [1990] reported AMPTE/CCE observations of compressional Pc5 pulsations that exhibited harmonically related transverse and compressional magnetic oscillations that modulated the flux of medium energy protons (E > 10 keV) with double frequency but did not discuss the event in detail. We report the first evidence for meridional sloshing of the equatorial node in the simultaneous compressional Pc5 pulsations and variations of electrons fluxes and electron densities observed by MagEIS and Hope, respectively. Figure 13 presents RBSP-A (left panel) and -B (right panel) electron fluxes for energies at 31.9 keV and 54.8 keV, electron densities and the Bz component of the magnetic field in FAC from 19:00 UT to 21:00 UT and at RBSP-B from 20:46 UT to 22:10 UT. The panels in the bottom of Figure 13 present expanded views of 20 min intervals with the double-frequency pulsations. The Bz component of the magnetic field varies with double frequencies out of phase with the fluxes of electrons and densities. This study gives better insight into the nodal structure of the waves and helps to clarify their source.

4.5. Testing Pc4-5 pulsation generation mechanisms

We tested several causes for the Pc4-5 pulsations, including solar wind pressure pulses, the KH instability on the magnetopause, drift-bounce resonant particle interactions, and the

mirror-mode instability. First, with the exception of the interval from 19:35 UT to 19:55 UT, the Wind observations shown in Figure 1 provide no evidence for periodic solar wind drivers in the Pc5 range, be they density variations or IMF fluctuations, thus ruling out solar wind pressure pulses as the direct cause of the Pc4-5 pulsations. We then considered the possibility of KH waves. These waves are expected when the solar wind velocity is high and both the magnetosheath and magnetospheric magnetic fields lie transverse to the magnetosheath flow, i.e. on the flanks of the magnetosphere when the IMF points southward or in particular northward [e.g., Guo et al., 2010]. As shown in Figure 1, the solar wind velocity during the interval when the Pc5 events occurred was only moderate, 400-460 km/s. Furthermore, the IMF did not point either strongly northward or southward. Therefore, we conclude that the compressional Pc5 pulsations were excited by processes internal to the magnetosphere.

Southwood [1981] and Kivelson and Southwood [1985] described how the resonant drift-bounce interaction of particles with an azimuthally-propagating wave generates large amplitude ULF waves in an inhomogeneous background field. For this to happen, the wave frequency ω must satisfy the resonance condition:

$$\omega - m\omega_d - N\omega_b = 0, \qquad (1)$$

where ω_d and ω_b are the angular drift and bounce frequencies, N is an integer, and m is the azimuthal wave number. Southwood [1973] predicted that particle flux oscillations just above and below the resonant energy should be 180° out of phase. As Figures 10a and b demonstrate, RBSP-A did not observe any such phase reversal in the electrons as a function of energy. We exclude the drift-bounce resonance as the cause of these compressional Pc5 pulsations.

Finally, we examined the mirror instability criterion. The mirror instability is a kinetic phenomenon that occurs spontaneously in anisotropic high β plasmas when the ratio of perpendicular to parallel pressures is large [Southwood and Kivelson, 1993]. The test for the mirror instability is approximately:

$$\Gamma = 1 + \beta_\perp [1 - T_\perp / T_{//}] < 0, \qquad (2)$$

where $T_{//,\perp}$ are the plasma temperatures parallel and perpendicular to the ambient magnetic field and $\beta_\perp$ is the ratio of the perpendicular component of the thermal plasma pressure to the magnetic pressure. For our calculations we obtained the magnetic field data from EMFISIS and thermal plasma pressures perpendicular and parallel to the magnetic field from RBSPICE. We used the density and temperature from HOPE to calculate the parallel and perpendicular thermal pressures within the energy range covered by this instrument, but found these pressures to be small compared to those from RBSPICE. Consequently, our calculations neglect the contributions from HOPE to the thermal pressures.

Figures 14a and b show RBSP-A and -B plasma and magnetic field parameters characterizing the pulsations. The upper panels indicate that magnetic field and plasma pressures vary in antiphase during the Pc5 pulsations. However, the total pressure is not balanced as might be expected for mirror mode waves. We suppose that this is because the RBSPICE (or even the RBSPICE + HOPE) plasma instruments do not observe the entire plasma distribution. Assuming that the total plasma pressure is proportional to the fraction that RBSPICE does observe, we scaled the thermal plasma pressures observed by RBSPICE upward to values that cause the sum of the magnetic and perpendicular thermal plasma pressure variations associated with the waves to be approximately constant during the intervals from 19:03 UT to 19:14 UT for RBSP-A and from 22:32 UT to 22:56 UT for RBSP-B. The upward scaling factors were 1.97 and 1.69, respectively. We then applied these factors to both the perpendicular and parallel pressures. The third panels of Figures 14a and b show the values of $\beta_\perp$ calculated from these scaled pressures. Shaded grey areas in the fourth panels show when the drift mirror instability is satisfied (< 0). As the test for the mirror instability is satisfied throughout most of the intervals of enhanced temperature (pressure) anisotropy and $\beta > 1$ at RBSP-A and -B, we attribute the compressional Pc5 pulsations observed on January 1, 2016 to the mirror instability.

Conclusions

We used Van Allen Probes and GOES multipoint magnetic field, electric field, plasma and energetic particle observations to study the nature of compressional Pc5 pulsations at the end of

a strong magnetic storm on January 1, 2016. From ~ 19:00 UT to 23:02 UT the magnetosphere was compressed and transient increases of the total magnetic field strength occurred every 20-40 min. During this interval the spacecraft observed compressional Pc 5 pulsations over a large longitudinal extent. The solar wind pressure enhancements initiated and/or amplified compressional wave activity in the dayside magnetosphere. The pulsations occupied the dayside magnetosphere from 5.26 to 6.6 Re and from 09:56 to 15:20 MLT. Successive solar wind pressure increases and magnetospheric compressions enhanced the amplitude of Pc5 wave activity to values from 10 to 16 nT. The strongest amplitudes occurred prior to local noon. They were observed when the IMF cone angle was less than 45^{o}. We studied the wave mode of the Pc5 pulsations and found that they had an antisymmetric structure.

The greatest spectral power densities observed at RBSP-A and -B occurred in the north/south, or Bz, component of the magnetic field at frequencies of ~4.5-6.0 mHz. The two spacecraft observed similar frequencies, indicating that conditions within the dayside magnetosphere remained steady for a long time and over a broad region. Enhanced spectral power densities at frequencies of ~22-29 mHz in the radial Bx component can be attributed to the simultaneous generation of poloidal Pc4 pulsations by a different mechanism. The frequencies of the Pc4 pulsations diminished with increasing radial distance. The dominant frequencies for the compressional Pc5 pulsations observed by GOES resembled those observed by RBSP-A and -B and we suppose that they were generated by the same sources. Pc4 pulsations observed by the GOES spacecraft displayed frequencies that were lower than those observed by RBSP-A and -B, since the GOES spacecraft were located further radially outward from Earth. Since the frequencies of the Pc4 pulsations depended on local time and radial distance from Earth, their sources must be more localized than those for the Pc5 pulsations.

When the spacecraft were in the vicinity of the geomagnetic equator, RBSP-A observed meridional sloshing of the equatorial wave node from Z_{SM} = 0.25 to 0.04 Re, while RBSP-B observed them from Z_{SM} = 0.19 to -0.08 Re. Consequently, we believe that the motion of the meridional oscillation of the position of the equatorial node was at least 0.15 to 0.18 Re. We

found that RBSP-A observed ratios near 1 at Z_{SM} = ~0.08 Re while RBSP-B observed ratios near 1 at Z_{SM} = ~0.10 Re. These were the locations where the southward-moving spacecraft RBSP-A and -B passed through the mean positions of the equatorial node at Z_{SM} = ~0.08 Re and at Z_{SM} = ~0.10 Re, respectively. We report the first evidence for meridional sloshing of the equatorial node in the double-frequency variations of electrons fluxes and electron density observed by MagEIS and HOPE, respectively.

The energetic particles observed by RBSP-A and -B showed a regular periodicity over a broad range of energies from tens of eV to 2 MeV with periods corresponding to those of the compressional component of the ULF magnetic field. The electron intensities exhibited quasi-periodic enhancements at all energies with the most intense at pitch angles near 90^{o}. The energetic electron fluxes oscillated out of phase with the magnetic field and did not display any phase shift across all energies. The depth of modulation was larger for higher energy electrons. We searched for possible solar wind triggers and discussed generation mechanisms for the compressional Pc5 pulsations in terms of drift mirror instability and drift bounce resonance. **We interpret the compressional Pc5 waves in terms of drift-mirror instability.**

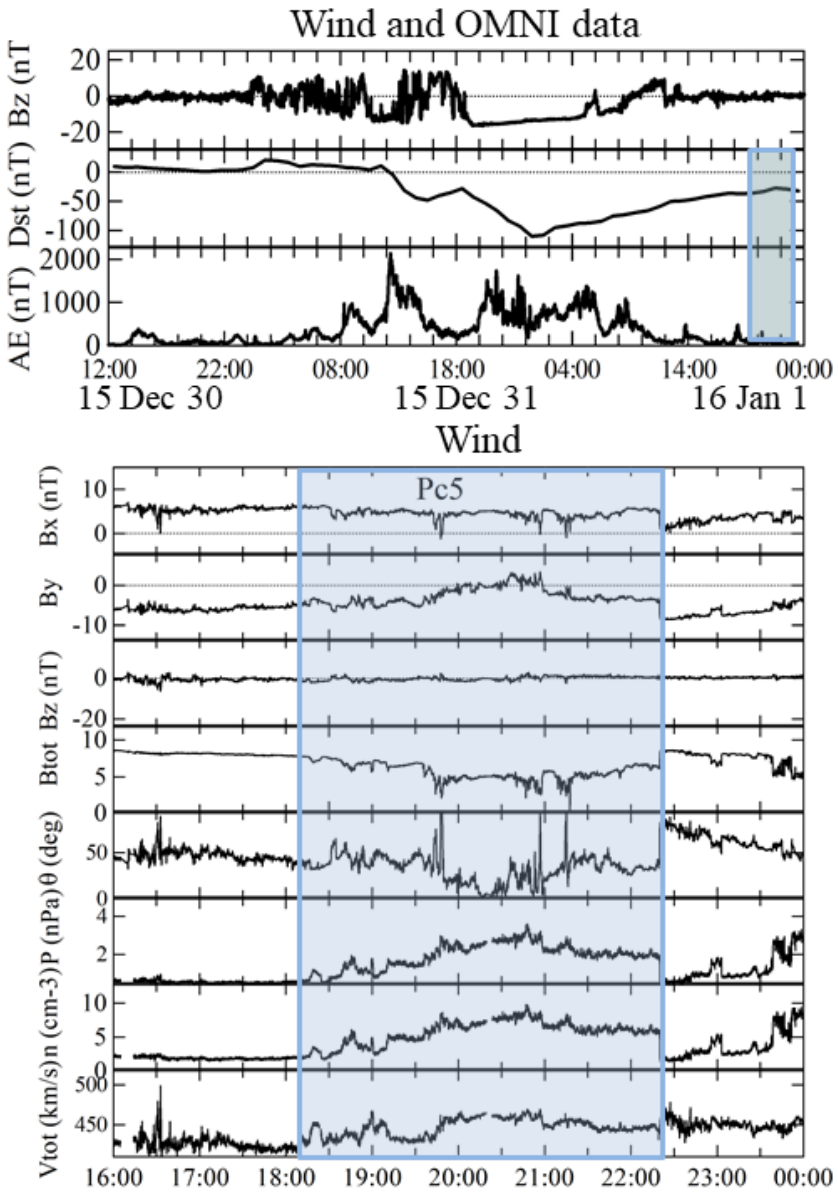

Figure 1. Bz component of the magnetic field observed at Wind, and geomagnetic activity Dst and AE indices obtained from the OMNI database (upper panels) from 12:00 UT on December 30 to 00:00 UT January 2, 2016. The bottom panels show Wind observations of the magnetic field components, total magnetic field strength, cone angle, pressure, plasma density, and velocity from 16:00 UT on January 1, 2016 to 00:00 UT on January 2. 2016. Shading highlights intervals when magnetospheric spacecraft observed Pc5 compressional pulsations.

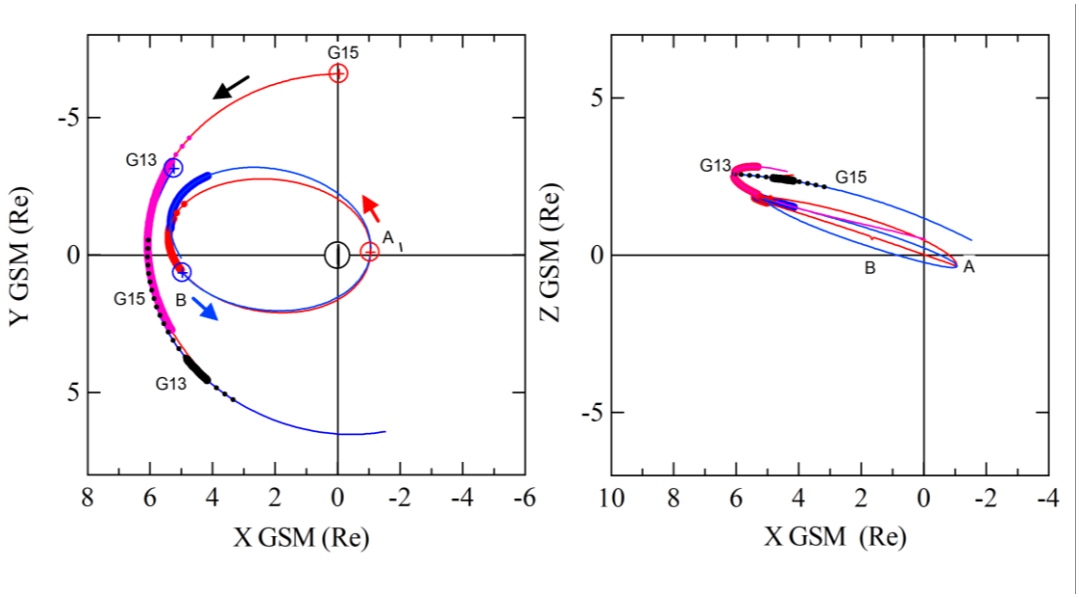

Figure 2. Trajectories of RBSP-A (red) and -B (blue) and G-13 (black) and -15 (purple) from 15:00 UT to 24:00 UT on January 1, 2016 in the X-Y and X-Z GSM planes. Open circles mark the beginning of the spacecraft trajectories which are duskward for the GOES spacecraft and duskward at apogee for the Van Allen Probes. The thick line segments indicate the locations of the spacecraft at the times when compressional Pc5 magnetic field pulsations occurred. Dots mark their locations where weak pulsations (A < 5 nT) occurred.

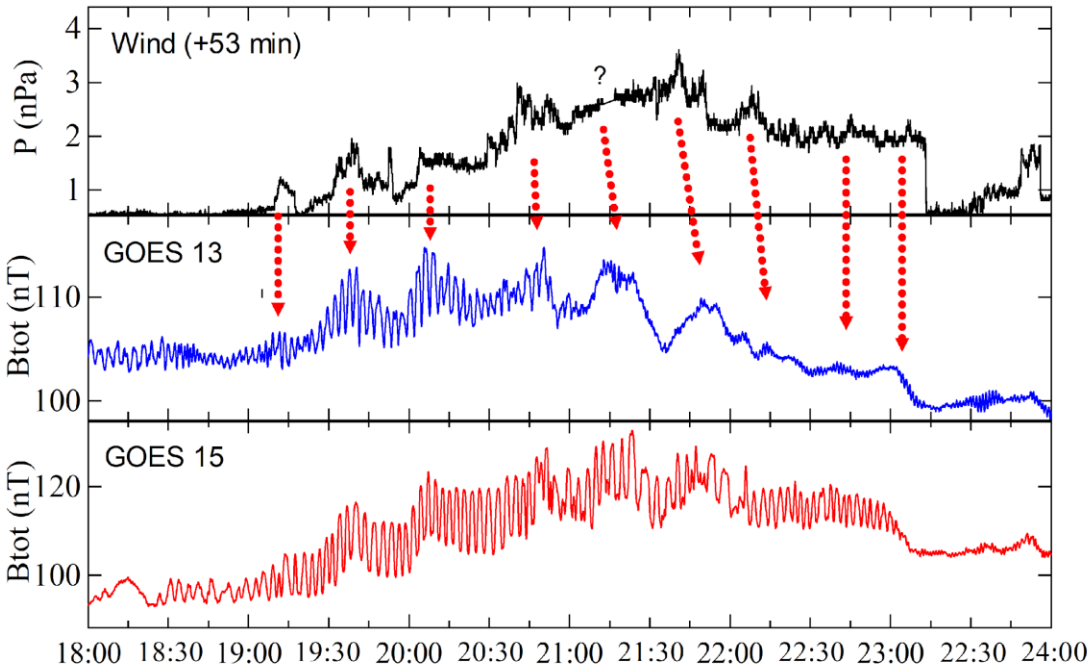

Figure 3. Observations of the solar wind dynamic pressure at Wind (time shifted) and the total magnetic field strength at G-13 and -15 from 18:00 UT to 24:00 UT. The arrows connect enhancements of the solar wind dynamic pressure to corresponding compressions of the magnetosphere.

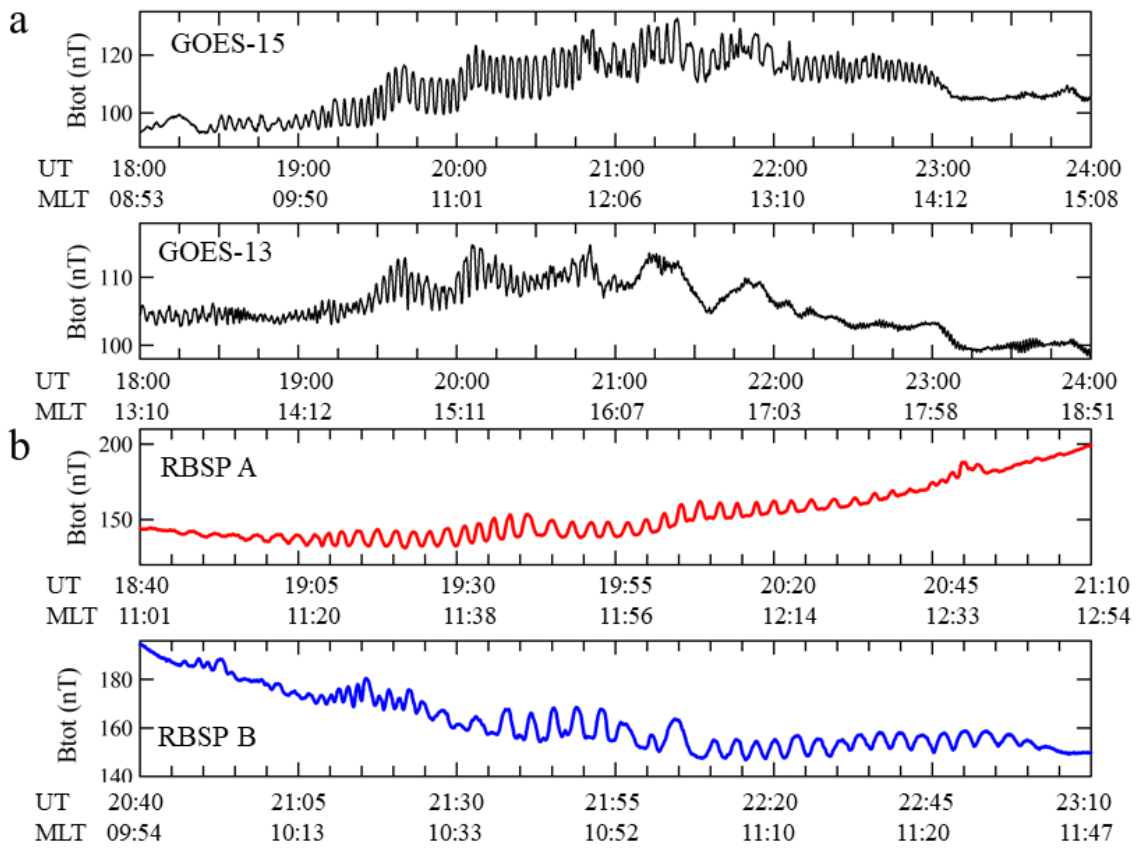

Figures 4 (a, b). G-15 and G-13 (a) total magnetic field strength from 18:00 UT to 24:00 UT on January 1, 2016. RBSP-A and -B (b) total magnetic field strength from 18:40 UT to 21:10 UT and from 20:40 UT to 23:10 UT on January 1, 2016, respectively, Beneath the panels are listed the universal time (UT) and magnetic local time (MLT).

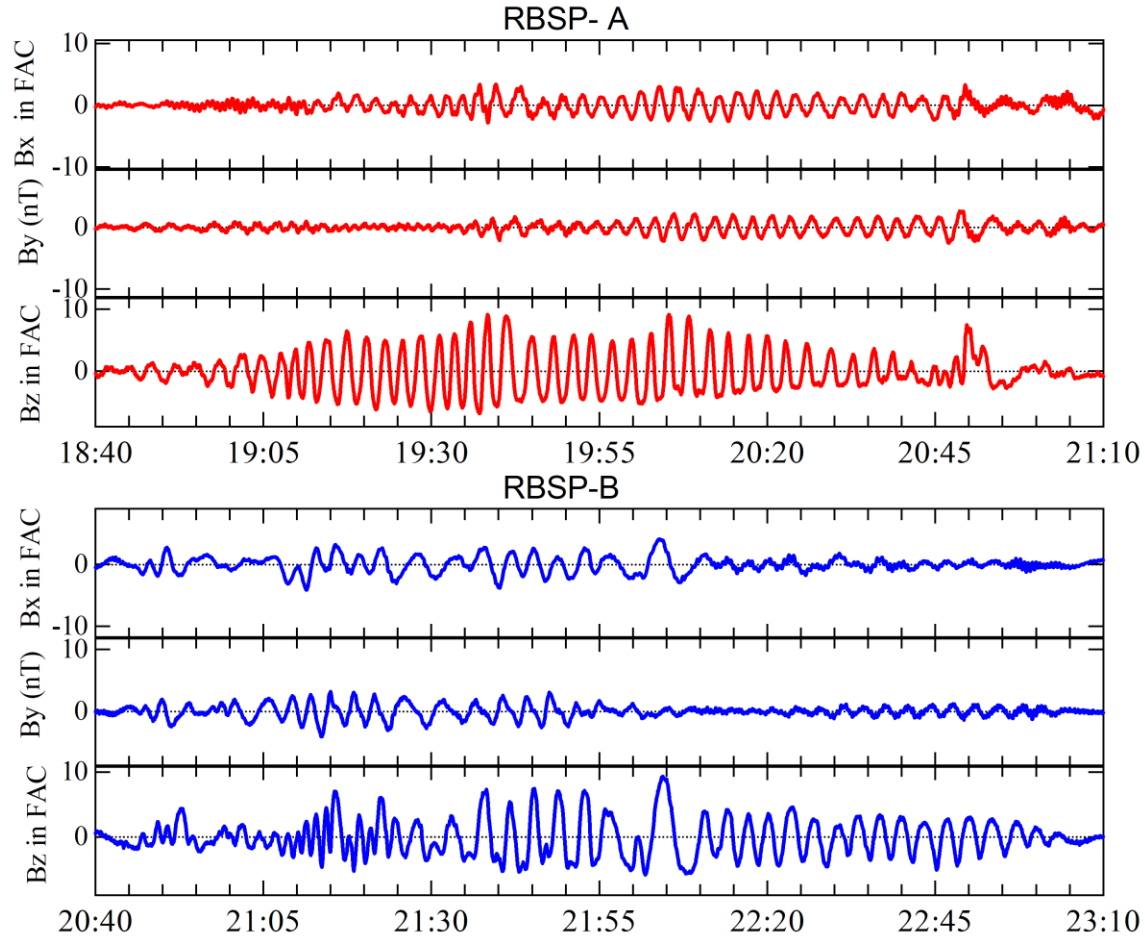

Figure 5. RBSP-A and -B magnetic field observations in field-aligned coordinates from 18:40 UT to 21:10 UT and from 20:40 UT to 23:10 UT on January 1, 2016, respectively.

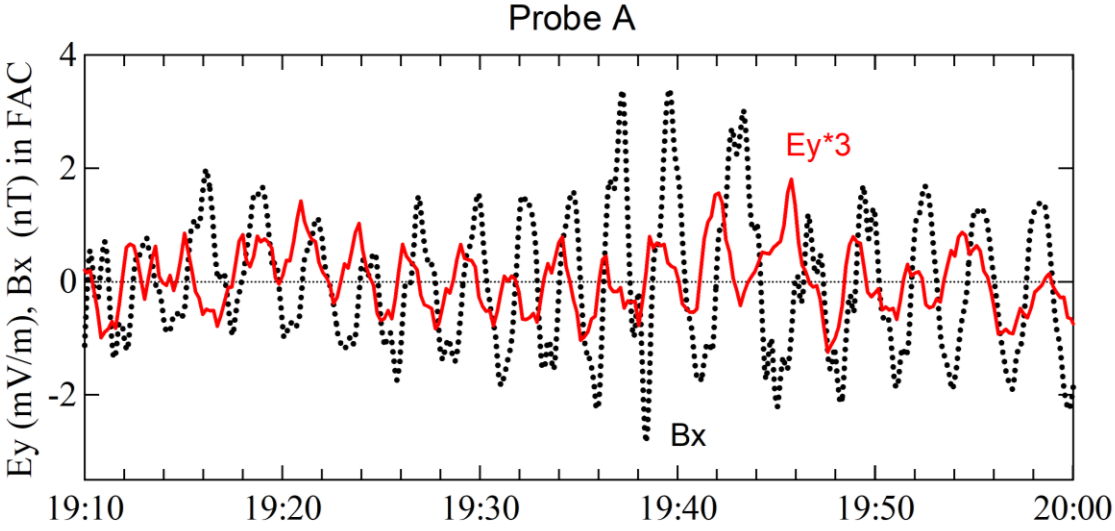

Figure 6. The phase difference between the RBSP-A azimuthal component of the electric field (red curve is boxcar smoothed**)** and the radial component of the magnetic field Bx in field-aligned coordinates (dashed curve) from 19:10 UT to 20:00 UT on January 1, 2016. The amplitude of Ey was multiplied by a factor of 3 to better display the visual effects.

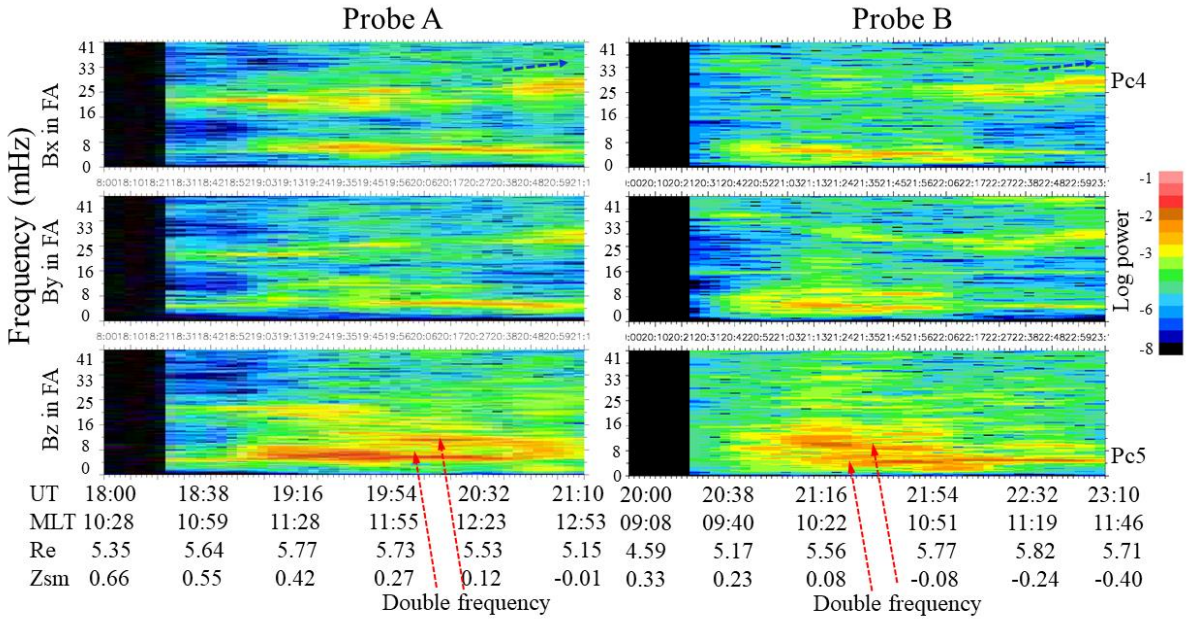

Figure 7. Three component dynamic spectra of magnetic field data at RBSP-A and -B from 18:00 to 21:10 UT and from 20:00 UT to 23:10 UT on January 1, 2016, respectively. Beneath the panels are listed the universal time (UT), magnetic local time (MLT), radius (Re) and Z (SM) in Earth radius.

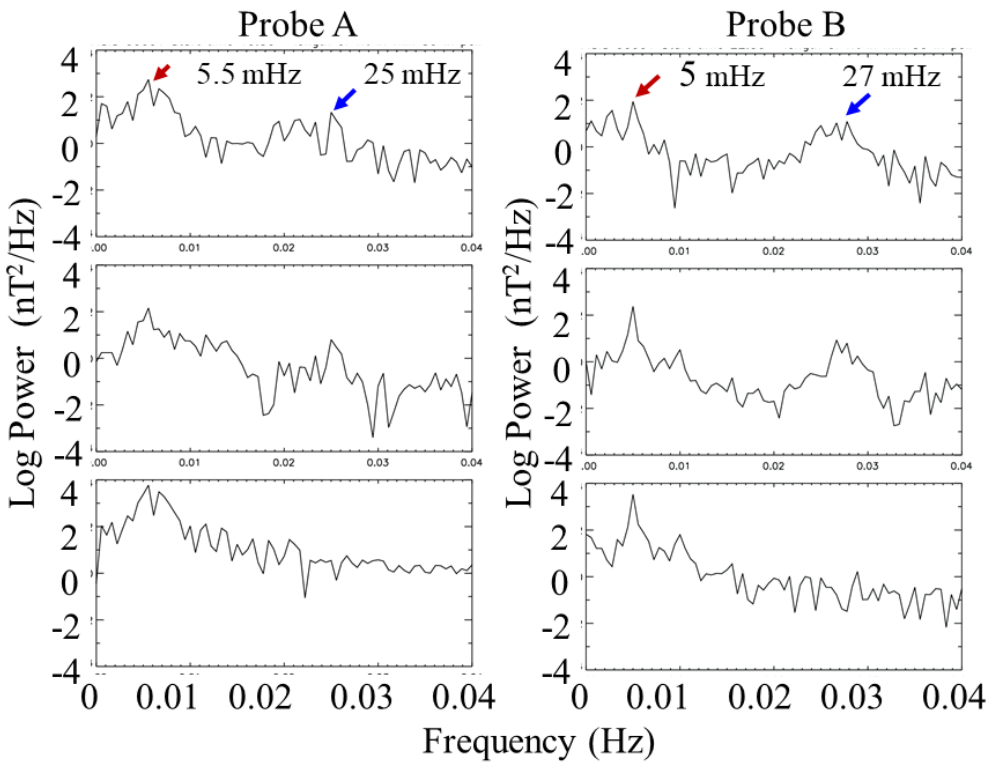

Figure 8. Fourier spectra calculated for the radial, azimuthal and compressional components of the RBSP-A and -B magnetic field in 5-minute sliding averaged mean field-aligned coordinates from 19:30 UT to 20:00 UT and from 22:30 UT to 23:00 UT on 1 January, 2016.

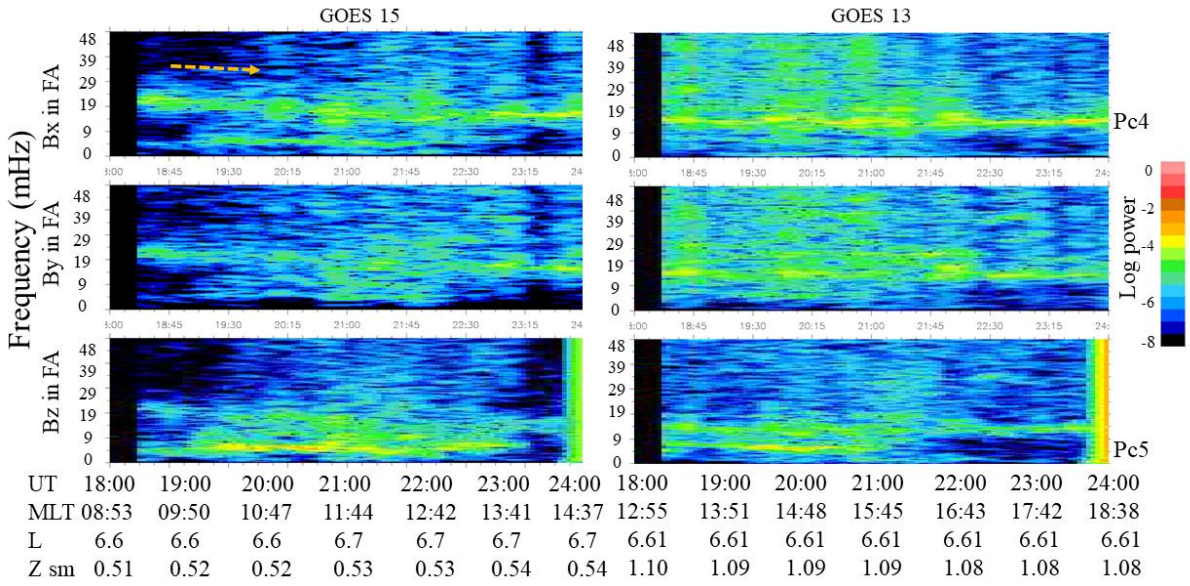

Figure 9. Three components of dynamic spectra of the magnetic field data at G-15 and G-13

from 18:00 UT to 24:00 UT on January 1, 2016. Beneath the panels are listed the universal time (UT), magnetic local time (MLT in SM), L and Z (SM) in Earth radii.

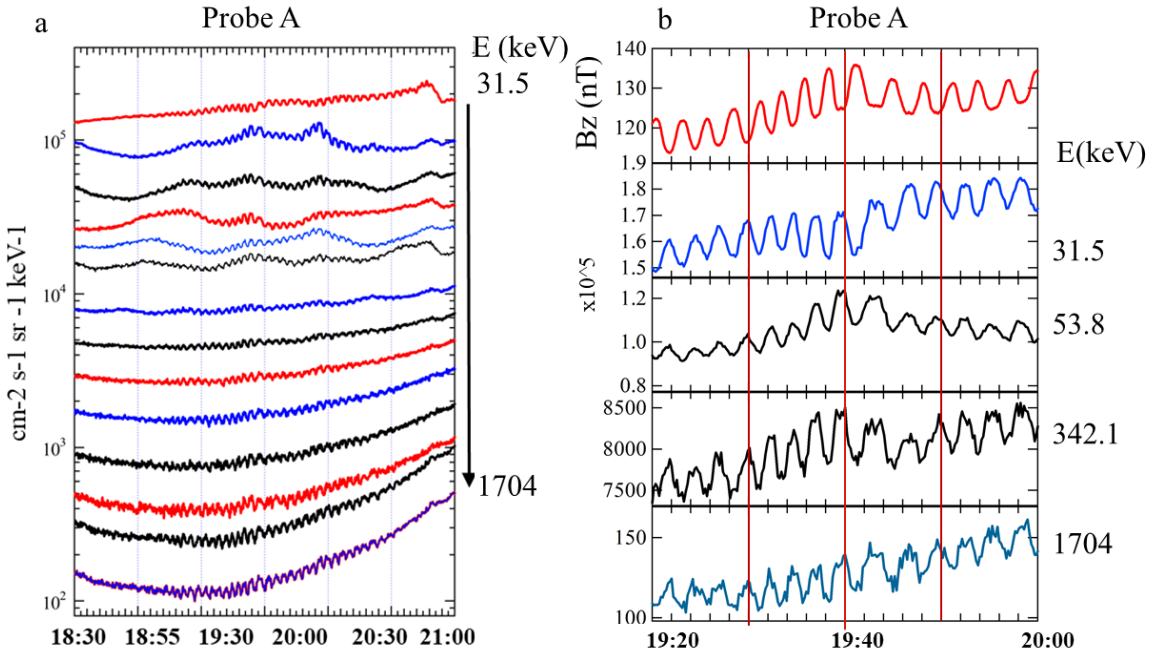

Figures 10 (a, b). RBSP-A observations of electron fluxes (a) in the energy range from 31.5 keV to 1704 keV from 18:30 UT to 21:00 UT and (b) their expanded view for selected energies from 19:20 UT to 20:00 UT.

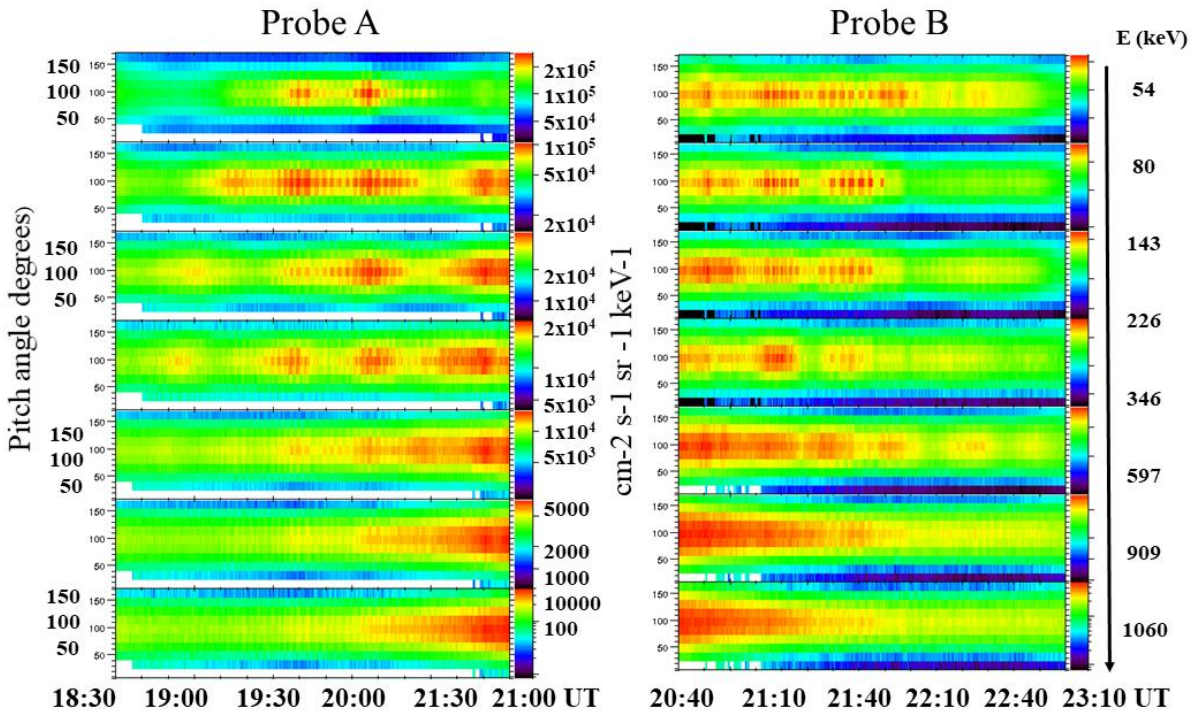

Figure 11. RBSP-A and -B observations of pitch-angle distributions for electrons in the energy range from 54 keV and 1060 keV from 18:30 to 21:00 UT and from 20:40 UT to 23:10 UT on January 1, 2016, respectively.

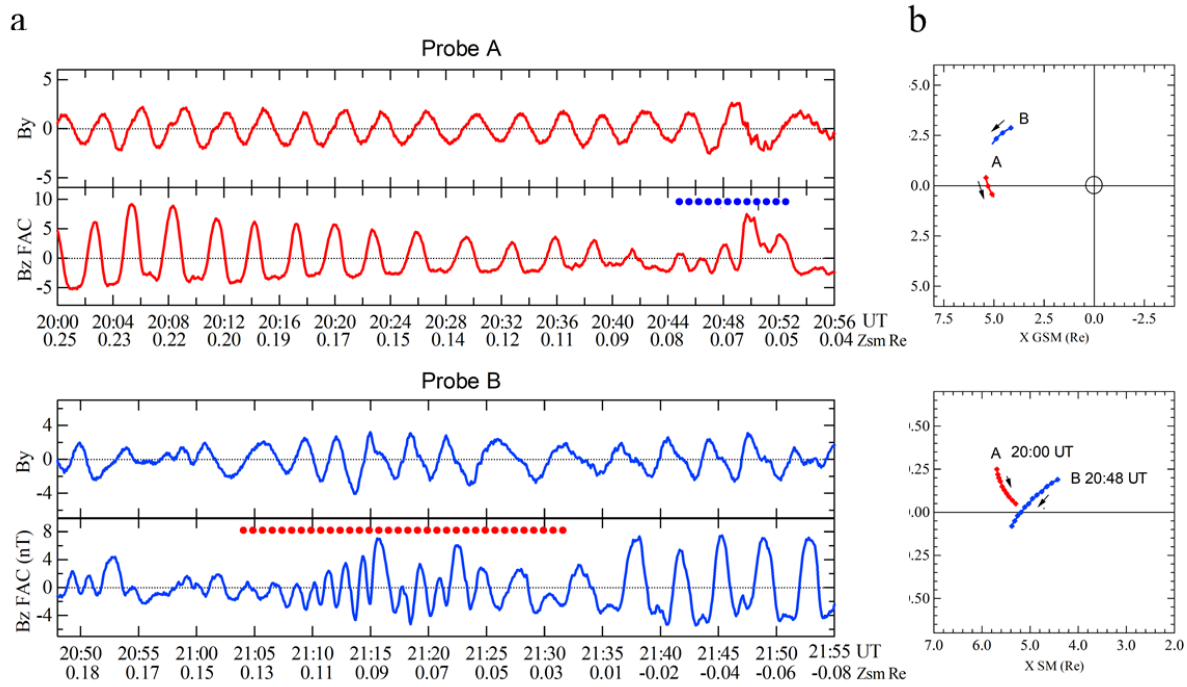

Figures 12 (a, b). RBSP-A and -B observations of double frequency pulsations (a) from 20:00 UT to 20:56 UT and from 20:48 UT to 21:55 UT, respectively, and (b) their locations in the X - Y GSM and X - Z SM planes. Red and blue dashed lines mark the intervals with harmonic structure of double-frequency pulsations.

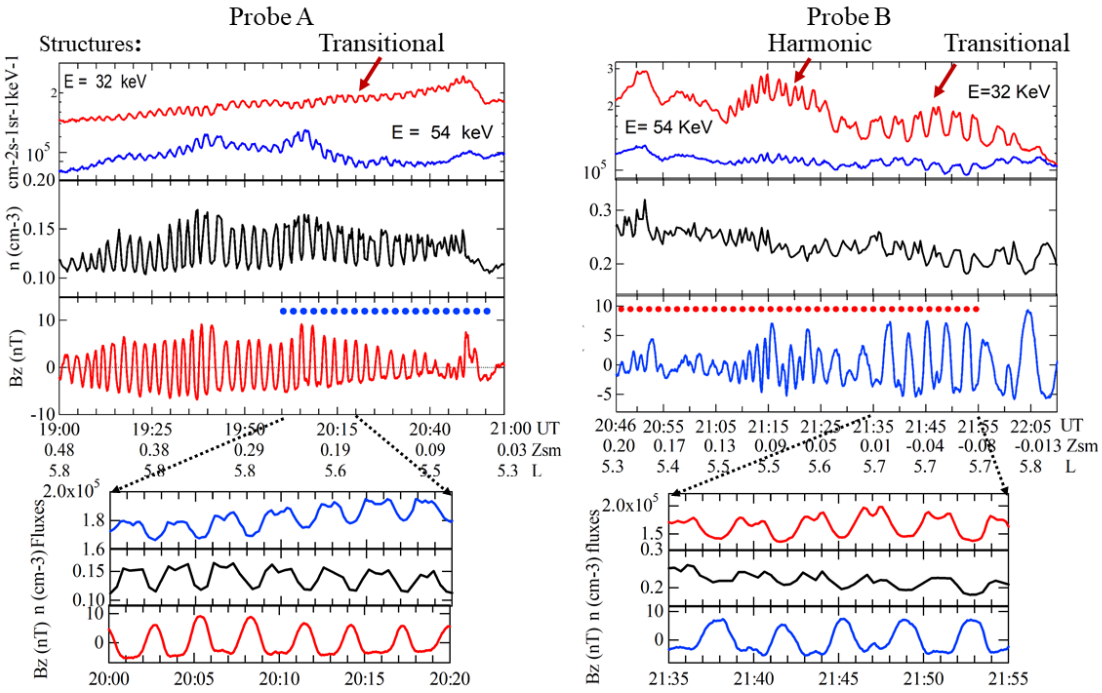

Figure 13. RBSP-A (left panel) and -B (right panel) presents electron fluxes for energies at 31.9 keV and 54.8 keV from EMFISIS, electron densities from HOPE and the Bz component of the magnetic field in field-aligned coordinates from MagEIS from 19:00 UT to 21:00 UT and from 20:46 UT to 22:10 UT, respectively. Dotted lines mark the intervals of observations of double-frequency pulsations. The panels in the bottom of the figure present expanded views of 20 min intervals with the double-frequency pulsations to better visualize their features.

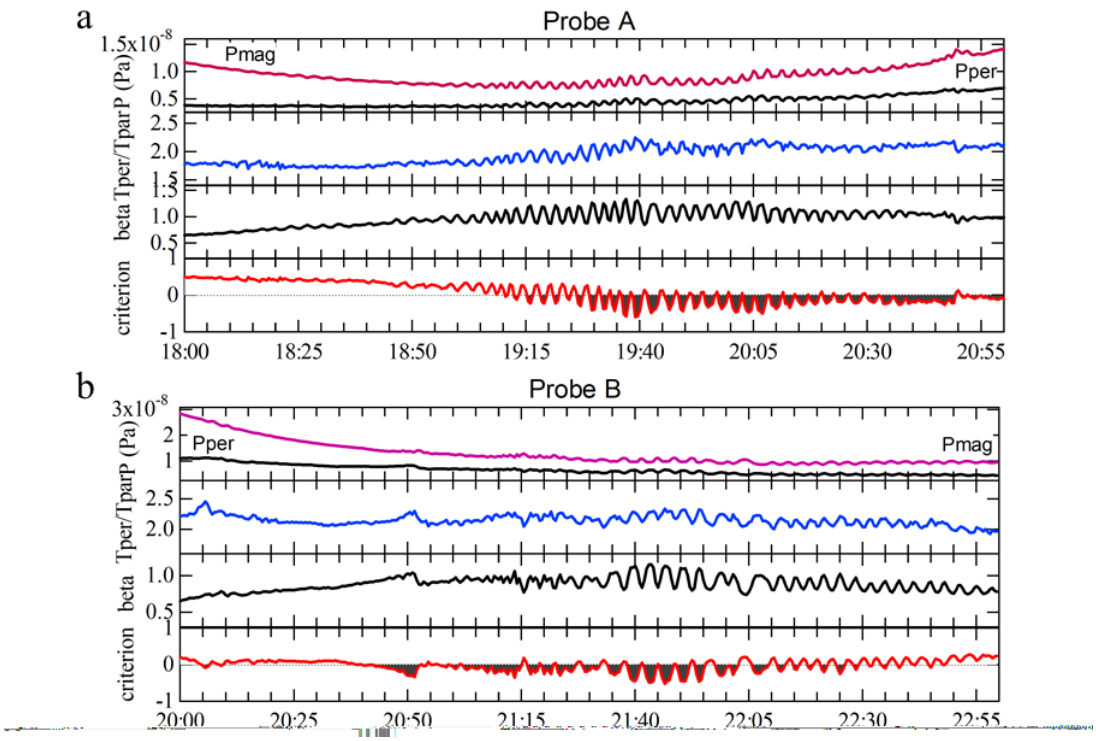

Figures 14 (a, b). RBSP-A and -B plasma and magnetic field parameters characterizing the pulsations. From top to bottom, the figure shows the magnetic pressure, perpendicular plasma pressure, the ratio of the plasma temperatures perpendicular and parallel to the magnetic field, beta, and the results for the mirror instability criterion on January 1, 2016. Shaded grey areas indicate the times when the drift mirror instability is satisfied (< 1).

Data availability. Data used in the paper are available publicly at http://cdaweb.gsfc.nasa.gov/istp_public/ (Coordinated Data Analysis Web, NASA, 2018). GOES data were obtained from http:// satdat.ngdc.noaa.gov/sem/goes/data/new_full/ (NOAA, 2018). The electric field data were obtained from http://www.space.umn.edu/ rbspefw-data (Wygant and Breneman, 2017).

Author contributions. GK drafted and wrote the paper with participation of all coauthors. DS conceived ideas, ME, ST, HS, CK –consulting regarding the data analysis, RR – software development, MB–consulting regarding drift mirror instability test.

Competing interests. The authors have no conflict of interest.

Acknowledgements. The Van Allen Probes mission is supported by NASA. NASA GSFC's CDAWEB provided Wind and GOES observations, while SSCWEB provided Van Allen Probes EPHEMERIS. GK was supported by NASA contract no 80NSSC19K0440. M. A. B. is grateful to the STFC (grant ST/R000697/1).